Journal of Thermal Analysis and Calorimetry (2020) 139:1345–1353
https://doi.org/10.1007/s10973-019-08501-4

Effectiveness of various shapes of Al_2O_3 nanoparticles on the MHD convective heat transportation in porous medium

CVFEM modelling

Dat D. Vo[1,2] · Mohammadali Hedayat[3] · Tehmina Ambreen[4] · Sabir A. Shehzad[5] · M. Sheikholeslami[6,7] · Ahmad Shafee[8] · Truong Khang Nguyen[1,2]

Received: 18 January 2019 / Accepted: 10 June 2019 / Published online: 20 June 2019

Abstract

The influences of Al_2O_3 nanoparticles with various shapes on thermal characteristics of nanofluid within a permeable space concerning magnetic force have been simulated by means of CVFEM. To form the final PDEs, radiation term has been incorporated. Impacts of magnetic force, radiation constraint, Rayleigh number and shape factor on nanomaterial behaviour have been analysed. Results demonstrate that the higher values of shape factor lead to augmented convective heat transfer. By augmenting the magnetic strength, conductive heat transfer can be predominant than that of the convection.

Keywords MHD · Nanoparticle's shape · Darcy law · Radiation · Nanofluid · CVFEM

✉ Sabir A. Shehzad
sabirali@cuisahiwal.edu.pk

Dat D. Vo
voduydat@tdtu.edu.vn

1 Division of Computational Physics, Institute for Computational Science, Ton Duc Thang University, Ho Chi Minh City, Vietnam

2 Faculty of Electrical and Electronics Engineering, Ton Duc Thang University, Ho Chi Minh City, Vietnam

3 J. Mike Walker '66 Department of Mechanical Engineering, Texas A&M University, College Station, USA

4 School of Mechanical Engineering, Kyungpook National University, Daegu 41566, South Korea

5 Department of Mathematics, COMSATS University Islamabad, Sahiwal 57000, Pakistan

6 Department of Mechanical Engineering, Babol Noshirvani University of Technology, Babol, Iran

7 Renewable Energy Systems and Nanofluid Applications in Heat Transfer Laboratory, Babol Noshirvani University of Technology, Babol, Iran

8 Applied Science Department, College of Technological Studies, Public Authority of Applied Education and Training, Shuwaikh, Kuwait

Introduction

Because of simplicity, cost-effectiveness and low noise of free convection, this mode can affect thermal behaviour of a wide range of engineering equipment. The natural convection mechanism transpires under the impact of the magnetic field in multiple processes including metal casting, the liquid cooling blanket of the fusion reactors and crystal growth. However, the existence of Lorentz force imposes an adverse effect on the phenomenon and deteriorates the convective flow. In an investigation of free convection within a cavity under magnetic field influence, Rudraiah [1] observed that the stronger Hartmann destroys the convective heat transportation rate and this suppression is more characteristic in the regions of the low Grashof number. Kakarantzas et al. [2] investigated liquid metal MHD flow inside a container and reported that the implication of Hartmann flow deteriorates nanomaterial velocity. In a similar way, Selimefendigil and Oztop [3] and Sheikholeslami [4] demonstrated an inverse association between the Lorentz force and Nusselt number.

In the above-mentioned scenarios, the undesirable impact of Hartmann number on free convection can be compensated to some extent by replacing the conventional coolants with the metallic nanofluids [5–9]. The term nanofluid is expressed for the colloidal solution of the traditional fluids and the nano-sized metallic or non-metallic particles exhibiting superior thermal behaviour than that of the hosting fluid and the suspended particles [10]. The magnetohydrodynamic (MHD) natural convection of the nanofluids for multiple operating conditions and nanofluid combinations has been presented by several studies. Sheremet et al. [11] analysed the MHD water–Cu nanofluid in a wavy enclosure under the influence of an isothermal corner heater. Kefayati [12, 13] implemented the FDLBM to scrutinize nanomaterial-free convection through a square cavity. Using the numerical approach, Sheikholeslami et al. [14–18] studied MHD and EHD convective transportation of water-based nanomaterials in a square enclosure, concentric annulus, semi-annulus and cubic cavity.

Fewer reports presented the MHD convective transportation within porous media. The permeable media possesses the advantages of the low density and large area for the optimal heat transfer. Selimefendigil and Oztop [19] scrutinized vented enclosure influenced by Lorentz forces to analyze mixed convection. Rashad et al. [20] explored the mutual impact of the internal heat generation and Lorentz forces on free convective flow of the copper–water within a rectangular tank. Finding new carrier fluid with greater thermal properties has been scrutinized by several researchers [21–33].

The objective of this investigation is to scrutinize study the impact of the nanoparticle shape variation on the MHD-free convection and the radiation of the Al_2O_3–water nanomaterial within a porous medium by implementing the CVFEM approach. The considered radiation parameter, shape factor, Hartmann number and particle volume fraction ranges are $0 \le \mathrm{Rd} \le 0.8$, $3 \le m \le 5.7$, $0 \le \mathrm{Ha} \le 20$ and $0\% \le \varphi \le 5\%$ respectively.

Formulation of problem and simulation

In the present problem, the impact of Hartmann flow on the behaviour of nanomaterial in a permeable geometry has been emphasized. CVFEM has been employed concerning triangular element. The imposed boundary conditions have been also depicted in Fig. 1. In order to model the porous terms, the Darcy law has been implemented. Shape factor influences on nanomaterial properties have been modelled. The problem under consideration has below equations:

$$\frac{\partial v}{\partial y} + \frac{\partial u}{\partial x} = 0 \tag{1}$$

$$\frac{\mu_{\mathrm{nf}}}{K} u = -\frac{\partial P}{\partial x} + \sigma_{\mathrm{nf}} B_0^2 \left[(\sin\gamma) v (\cos\gamma) - u (\sin\gamma)^2 \right] \tag{2}$$

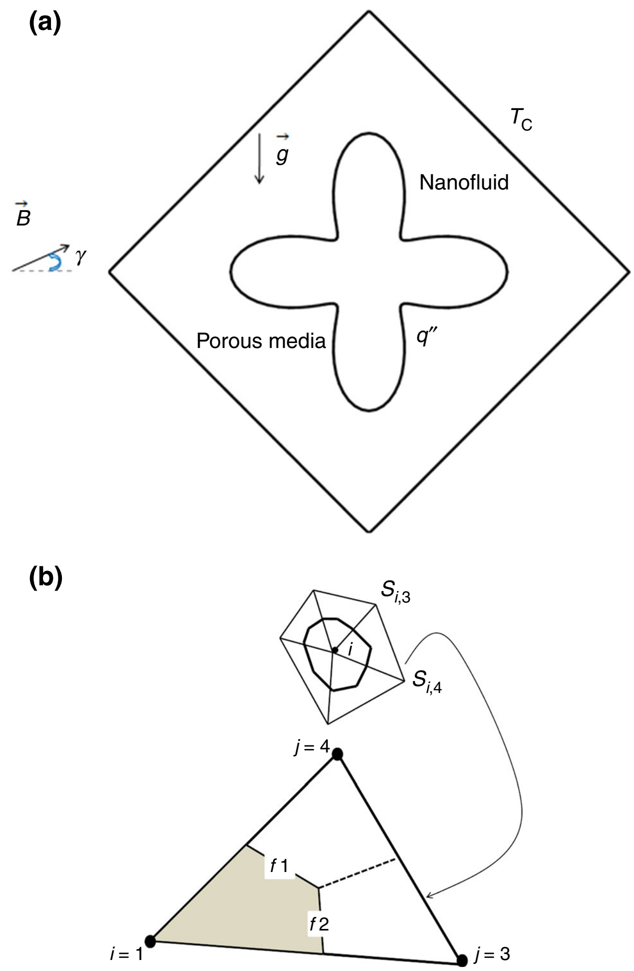

Fig. 1 **a** Current porous domain, **b** CVFEM element

$$\frac{\mu_{\mathrm{nf}}}{K} v = -\frac{\partial P}{\partial y} + (T - T_{\mathrm{c}}) g \rho_{\mathrm{nf}} \beta_{\mathrm{nf}} + \sigma_{\mathrm{nf}} B_0^2 (\cos\gamma) [(\sin\gamma) u - (\cos\gamma) v] \tag{3}$$

$$\frac{1}{(\rho C_{\mathrm{p}})_{\mathrm{nf}}} \frac{\partial q_{\mathrm{r}}}{\partial y} + \left(u \frac{\partial T}{\partial x} + v \frac{\partial T}{\partial y} \right) = k_{\mathrm{nf}} (\rho C_{\mathrm{p}})_{\mathrm{nf}}^{-1} \left(\frac{\partial^2 T}{\partial y^2} + \frac{\partial^2 T}{\partial x^2} \right), \left[T^4 \cong 4 T_{\mathrm{c}}^3 T - 3 T_{\mathrm{c}}^4, q_{\mathrm{r}} = -\frac{4\sigma_{\mathrm{e}}}{3\beta_{\mathrm{R}}} \frac{\partial T^4}{\partial y} \right] \tag{4}$$

The thermophysical properties of nanomaterial were estimated by the below equations

$$(\rho C_{\mathrm{p}})_{\mathrm{nf}} / (\rho C_{\mathrm{p}})_{\mathrm{f}} = PP, \quad PP = (1 - \phi) + \phi (\rho C_{\mathrm{p}})_{\mathrm{s}} / (\rho C_{\mathrm{p}})_{\mathrm{f}} \tag{5}$$

$$(\rho\beta)_{\mathrm{nf}} = (\rho\beta)_{\mathrm{f}} (1 - \phi) + \phi (\rho\beta)_{\mathrm{s}} \tag{6}$$

$$\rho_{\mathrm{nf}} - \phi \rho_{\mathrm{s}} = (1 - \phi) \rho_{\mathrm{f}} \tag{7}$$

$$1 + A = \sigma_s/\sigma_f, \frac{\sigma_{nf}}{\sigma_f} = B, \quad B - 1 = 3\phi \frac{A}{A + 3 - \phi A} \tag{8}$$

The effective viscosity μ_{nf} as involving Brownian motion:

$$\mu_{eff} = \left([1-\phi]^{-2.5} + \frac{k_{Brownian}}{\Pr_f k_f}\right)\mu_f$$
$$g'(d_p, \phi, T) = gg$$
$$k_{Brownian} = 5 \times 10^4 c_{p,f}\, gg\, \rho_f \phi \sqrt{\frac{\kappa_b T}{\rho_p d_p}}$$
$$gg = \mathrm{Ln}(T)\big(a_1 + a_3\mathrm{Ln}(\phi) + a_4\mathrm{Ln}(d_p)\mathrm{Ln}(\phi) + a_2\mathrm{Ln}(d_p) + a_5\mathrm{Ln}(d_p)^2\big) + \big(a_6 + \mathrm{Ln}(d_p)a_{10}\mathrm{Ln}(d_p) + a_8\mathrm{Ln}(\phi) + a_9\mathrm{Ln}(d_p)\mathrm{Ln}(\phi) + a_7\mathrm{Ln}(d_p)\big) \tag{9}$$

The impact of the nanoparticle shape factor has been involved in the estimation of the effective thermal conductivity k_{nf} as:

$$k_p - k_f = \mathrm{kr}, \quad \frac{k_{nf}}{k_f} = \frac{\mathrm{kr}\, m\phi + k_f + \mathrm{kr}\,\phi + mk_f + k_p}{k_p + m\,k_f + kr\,\phi + k_f} \tag{10}$$

The various shape factors, related coefficient and properties are enlisted in Tables 1–3 [34].

Equation (11) has been considered to attain the dimensionless form.

$$(y,x) = (Y,X)L, \Psi = \psi/\alpha_{nf}, \; \theta = \frac{T - T_c}{\Delta T}, \Delta T k_f L^{-1} = q'' \tag{11}$$

The final expression can be written as:

$$\frac{\partial^2\Psi}{\partial X^2} + \frac{\partial^2\Psi}{\partial Y^2} = -\mathrm{Ha}\frac{A_6}{A_5}\left[(\cos\gamma)\frac{\partial^2\Psi}{\partial X^2}(\cos\gamma) + 2\frac{\partial^2\Psi}{\partial X\,\partial Y}(\sin\gamma)(\cos\gamma) + \frac{\partial^2\Psi}{\partial Y^2}(\sin^2\gamma)\right] - \frac{A_3 A_2}{A_4 A_5}\frac{\partial\theta}{\partial X}\mathrm{Ra} \tag{12}$$

$$\left(\frac{\partial^2\theta}{\partial X^2}\right) + \left(1 + \frac{4}{3}\left(\frac{k_{nf}}{k_f}\right)^{-1}\mathrm{Rd}\right)\frac{\partial^2\theta}{\partial Y^2} = -\frac{\partial\Psi}{\partial X}\frac{\partial\theta}{\partial Y} + \frac{\partial\theta}{\partial X}\frac{\partial\Psi}{\partial Y} \tag{13}$$

In two recent equations, the definition of new parameters is:

$$\mathrm{Ha} = \frac{\sigma_f K B_0^2}{\mu_f}, \; \mathrm{Ra} = \frac{g\,K\,(\rho\beta)_f L\,\Delta T}{\mu_f\,\alpha_f}, \; \mathrm{Rd} = 4\sigma_e T_c^3/(\beta_R k_f)$$
$$A_1 = \frac{\rho_{nf}}{\rho_f}, \quad A_2 = \frac{(\rho C_P)_{nf}}{(\rho C_P)_f}, \quad A_5 = \frac{\mu_{nf}}{\mu_f},$$
$$A_3 = \frac{(\rho\beta)_{nf}}{(\rho\beta)_f}, \quad A_6 = \frac{\sigma_{nf}}{\sigma_f}, \quad A_4 = \frac{k_{nf}}{k_f} \tag{14}$$

In addition, the boundaries are summarized as:

$$\theta = 0.0 \quad \text{on outer surfaces}$$
$$\Psi = 0.0 \quad \text{all boundaries}$$
$$\frac{\partial\theta}{\partial n} = 1.0 \quad \text{on inner surface} \tag{15}$$

To calculate Nu_{loc} and Nu_{ave}, the below equations were employed:

Table 1 The coefficient values of Al_2O_3–water nanofluid

Coefficient values	Al_2O_3–water
a_1	52.813488759
a_2	6.115637295
a_3	0.6955745084
a_4	4.17455552786E−02
a_5	0.176919300241
a_6	− 298.19819084
a_7	− 34.532716906
a_8	− 3.9225289283
a_9	− 0.2354329626
a_{10}	− 0.999063481

Table 3 Different values of m

Platelet	Brick	Cylinder	Spherical	Shape
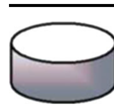	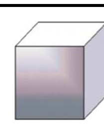		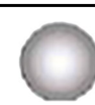	
5.7	3.7	4.8	3	m

Table 2 Thermophysical properties of water and nanoparticles

	$\rho/\mathrm{kg\,m^{-3}}$	$C_p/\mathrm{J\,kgK^{-1}}$	$k/\mathrm{W\,m\,K^{-1}}$	$\beta \times 10^5/\mathrm{K^{-1}}$	$\sigma/\Omega\,\mathrm{m^{-1}}$
Water	997.1	4179	0.613	21	0.05
Al_2O_3	3970	765	25	0.85×10^{-5}	1×10^{-10}

Table 4 Variation of Nu_{ave} with change of mesh size at $Ra = 600, Rd = 0.8, Ha = 20$ and $\phi = 0.04$.

Mesh size in radical direction × angular direction				
51 × 151	61 × 181	71 × 211	81 × 241	91 × 271
1.777101	1.7797347	1.783917	1.784450	1.7860465

Table 5 Variation of Nu_{ave} at Pr = 0.733

Ha	$Gr = 2 \times 10^5$	
	Present	Rudraiah et al. [1]
50	2.67911	2.8442
10	4.9047	4.8053

$$Nu_{loc} = \frac{1}{\theta}\left(1 + \frac{4}{3}\left(\frac{k_{nf}}{k_f}\right)^{-1} Rd\right)\left(\frac{k_{nf}}{k_f}\right) \tag{16}$$

$$Nu_{ave} = \frac{1}{S}\int_0^s Nu_{loc}\, ds \tag{17}$$

Sheikholeslami [34] is the pioneer of CVFEM. This technique combines FEM and FVM and uses the benefits of both approaches. In the final step, the Gauss–Seidel technique has been applied to find the values of scalars in each corner of triangular element. Various improvements in numerical approaches have been reported in recent decade [35–47].

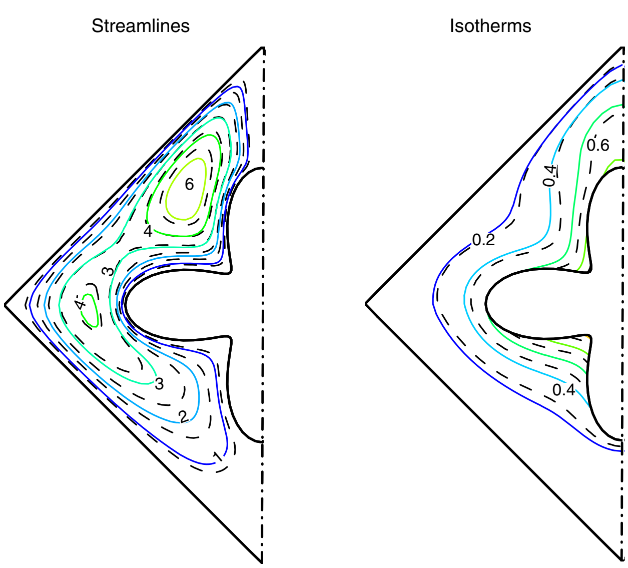

Fig. 2 Impacts of ϕ on nanofluid behaviour ($\phi = 0.04$ (—) and $\phi = 0$ (- - -)) when $Ra = 600, Ha = 0, m = 5.7, Rd = 0.8$

In order to attain mesh insensitive results, a mesh analysis has been conducted for all the states. Table 4 is an example which demonstrates the results of various mesh sizes for a certain case. Furthermore, to ensure the correctness of the written code, the outputs have been compared with the previously published studies [1] which employed the same code. Table 5 validates that the present results are in reasonable accordance with the past literature. In addition, other validation exists in Refs. [48, 49].

Results and discussion

In the present investigation, the role of nanoparticle shape on the transportation of nanomaterial within porous tank with employing buoyancy and radiation parameters was depicted. To control the velocity, magnetic force was involved. The results have been analysed to predict the impact of the radiation parameter ($0 \le Rd \le 0.8$), shape factor ($3 \le m \le 5.7$), Hartmann number ($0 \le Ha \le 20$) and concentration ($0\% \le \varphi \le 5\%$) of the alumina nanoparticles.

Figure 2 illustrates the impact of platelet-shaped ($m = 5.7$) nanoparticles addition ($\varphi = 4\%$) on the streamlines and the isotherm profiles of the porous medium at Ra = 600 and Rd = 0.8 without magnetic field effect. It is evident that the convective coefficient reduces while the Ψ_{max} augments with the introduction of the nanomaterial within hosting fluid because k_{nf} is greater than k_f. The impact of the Hartmann number on the nanofluid migration at Rd = 0.8, m = 5.7, φ = 4% for the $Ra = 100$ and $Ra = 600$ is illustrated in Figs. 3 and 4. The impact of the Lorentz forces results in the augmentation of temperature surface. The fluid convection incites a clockwise recirculating eddy which is subdivided into the bottom and top sections of the cavity, and this division is more perceptible at lower Ra and higher Ha. Lorentz forces results in the augment of Ψ_{max}. The mode of heat transfer is conductive at lower Ra, while it is relatively convective at the higher Ra.

The dependence of Nu_{avg} on the shape factor (m), (Rd), (Ha) have been shown in Fig. 5. Results show that Nu_{avg} observes the direct dependence on the m. The platelet shapes ($m = 5.7$) demonstrated the best performance of all the selected nanoparticle shapes followed by cylindrical ($m = 4.8$)-, brick ($m = 3.7$)- and spherical ($m = 3$)-shaped particles. Like m, the Rd also demonstrates a direct relationship with the Nu_{avg}. However, compared to the m, Ra and the Ha, the results of Nu_{avg} are more sensitive towards the variation of the Rd. The trend of the Nu_{avg} is also

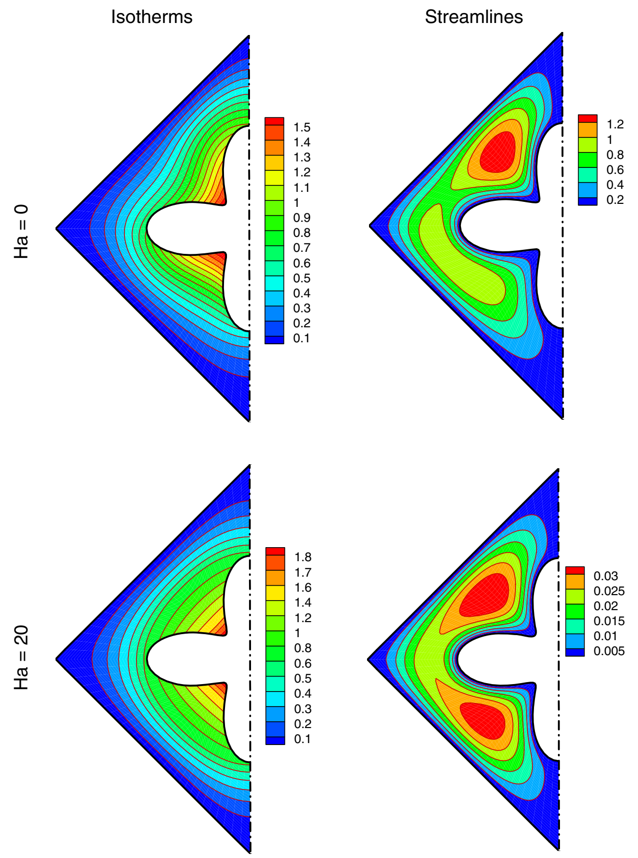

Fig. 3 Impacts of Ha on nanofluid flow when $\mathrm{Ra} = 100, \mathrm{Rd} = 0.8, m = 5.7, \phi = 0.04$

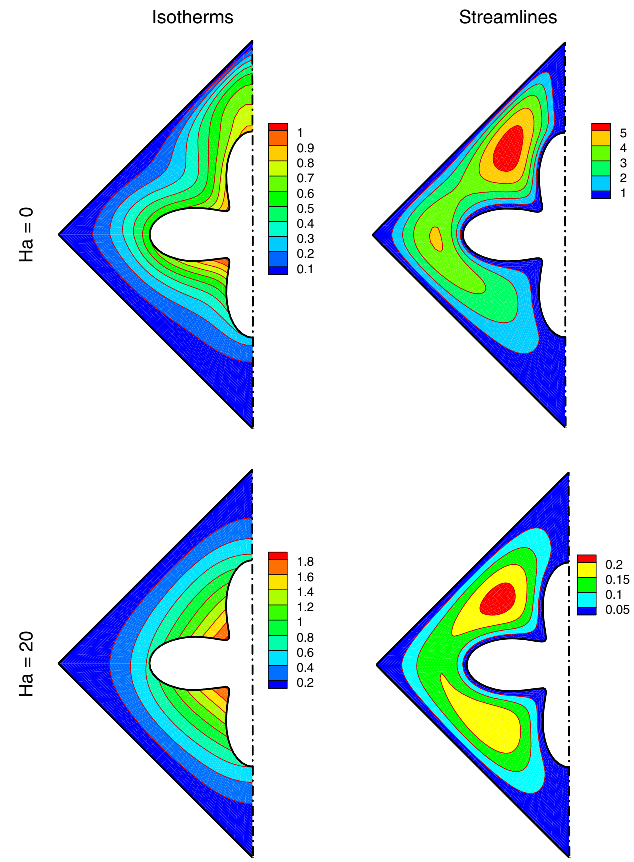

Fig. 4 Impacts of Ha on nanofluid flow when $\mathrm{Ra} = 600, \mathrm{Rd} = 0.8, m = 5.7, \phi = 0.04$

ascending as a function of the Ha and Ra; however, for the conditions of constant a Rd , m and φ, the $\mathrm{Nu}_{\mathrm{avg}}$ demonstrates declining trend with the increasing values of Ha and Ra. Based on the results, a correlation for the estimation of the $\mathrm{Nu}_{\mathrm{avg}}$ as a function of the considered parameter can be predicted as;

$$\begin{aligned}\mathrm{Nu}_{\mathrm{ave}} = {} & 1.86 + 0.042\,m + 0.64\,\mathrm{Rd} + 0.3\,\mathrm{Ra} - 0.25\,\mathrm{Ha} \\ & + 7 \times 10^{-3} m\,\mathrm{Ha} - 0.16\,\mathrm{Rd}\,\mathrm{Ha} - 0.3\,\mathrm{Ra}\,\mathrm{Ha} \\ & + 1.4 \times 10^{-4}\,\mathrm{m}^2\end{aligned} \tag{18}$$

The validly of the proposed correlation is applicable for the studied radiation parameter ($0 \leq \mathrm{Rd} \leq 0.8$), shape factor ($3 \leq m \leq 5.7$), nanomaterial concentration ($0\% \leq \varphi \leq 5\%$), Hartmann number ($0 \leq \mathrm{Ha} \leq 20$) and ($100 \leq \mathrm{Re} \leq 600$).

Conclusions

The manuscript investigates the influence of the nanomaterial shape variation on the MHD-free convection and the radiative heat transfers of the Al_2O_3–water nanomaterial within a porous medium by employing the CVFEM approach. The considered radiation parameter, shape factor, Hartmann number and particle volume fraction ranges are $0 \leq \mathrm{Rd} \leq 0.8$, $3 \leq m \leq 5.7$, $0 \leq \mathrm{Ha} \leq 20$ and $0\% \leq \varphi \leq 5\%$, respectively. The findings of the study can be concluded as:

- The higher shape factor augments the $\mathrm{Nu}_{\mathrm{ave}}$. The platelet shapes ($m = 5.7$) demonstrated the highest $\mathrm{Nu}_{\mathrm{avg}}$ followed by cylindrical ($m = 4.8$)-, brick ($m = 3.7$)- and spherical ($m = 3$)-shaped particles.
- Compared to the m, Ra and the Ha, the results of $\mathrm{Nu}_{\mathrm{ave}}$ are more sensitive towards the variation of the Rd. The convective mode is predominating when Ha = 0.

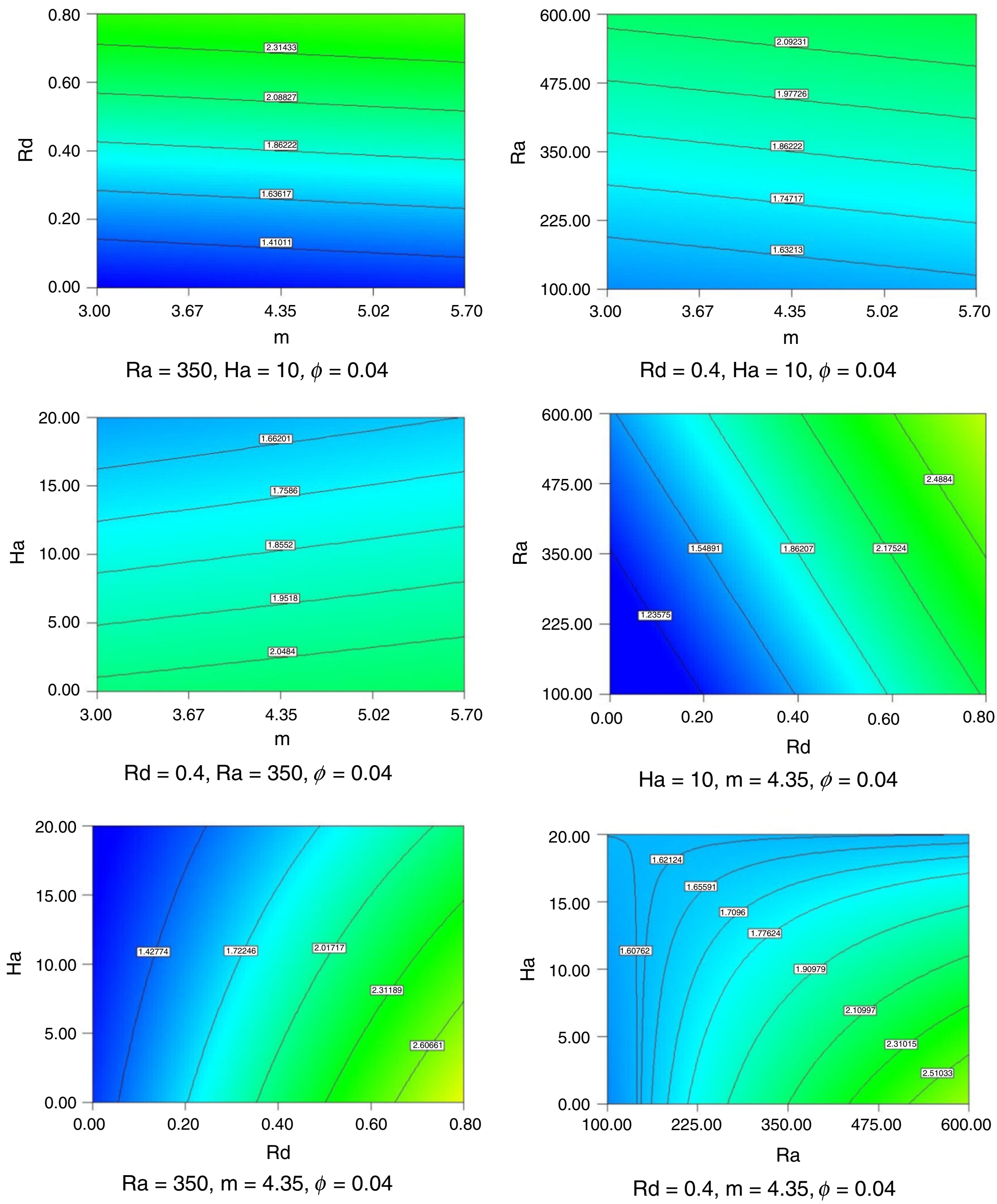

Fig. 5 Impacts of Ra, Ha, Rd, m, ϕ on $\mathrm{Nu}_{\mathrm{ave}}$

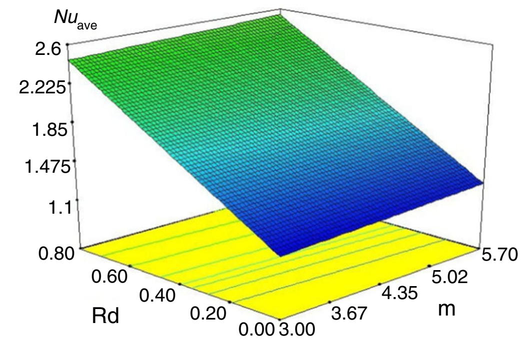

Ra = 350, Ha = 10, ϕ = 0.04

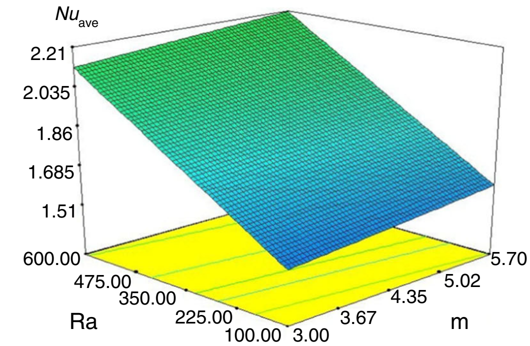

Rd = 0.4, Ha = 10, ϕ = 0.04

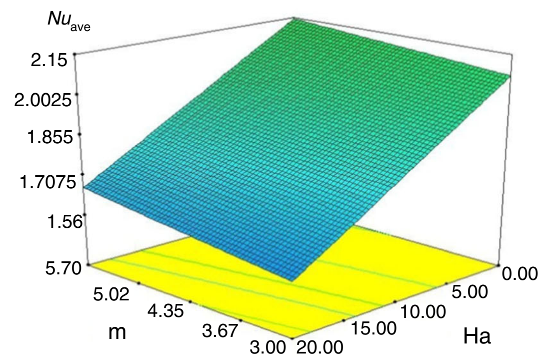

Rd = 0.4, Ra = 350, ϕ = 0.04

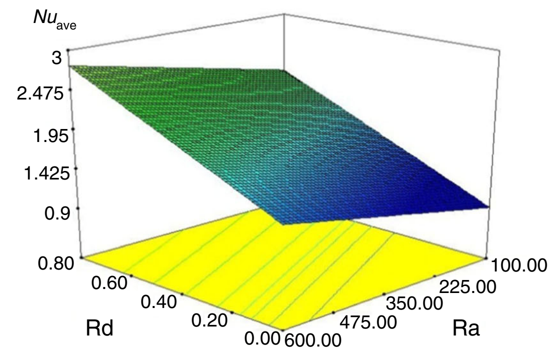

Ha = 10, m = 4.35, ϕ = 0.04

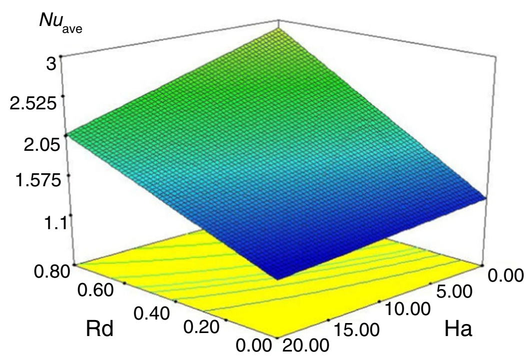

Ra = 350, m = 4.35, ϕ = 0.04

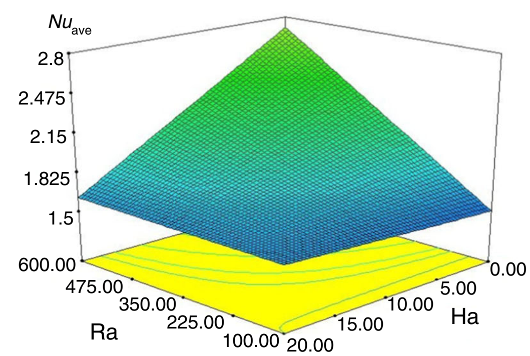

Rd = 0.4, m = 4.35, ϕ = 0.04

Fig. 5 continued

References

1. Rudraiah N, Barron RM, Venkatachalappa M, Subbaraya CK. Effect of a magnetic field on free convection in a rectangular enclosure. Int J Eng Sci. 1995;33:1075–84. https://doi.org/10.1016/0020-7225(94)00120-9.
2. Kakarantzas SC, Sarris IE, Grecos AP, Vlachos NS. Magnetohydrodynamic natural convection in a vertical cylindrical cavity with sinusoidal upper wall temperature. Int J Heat Mass Transf. 2009;52:250–9. https://doi.org/10.1016/j.ijheatmasstransfer.2008.06.035.
3. Selimefendigil F, Öztop HF. Corrugated conductive partition effects on MHD free convection of CNT-water nanofluid in a cavity. Int J Heat Mass Transf. 2019;129:265–77.
4. Sheikholeslami M. CuO-water nanofluid flow due to magnetic field inside a porous media considering Brownian motion. J Mol Liq. 2018;249:921–9.
5. Cao L, Si X, Zheng L. Convection of Maxwell fluid over stretching porous surface with heat source/sink in presence of nanoparticles: Lie group analysis. Appl Math Mech. 2016;37:433–42.

6. Selimefendigil F, Oztop HF. Forced convection and thermal predictions of pulsating nanofluid flow over a backward facing step with a corrugated bottom wall. Int J Heat Mass Transf. 2017;110:231–47.
7. Sheikholeslami M, Jafaryar M, Hedayat M, Shafee A, Li Z, Nguyen TK, Bakouri M. Heat transfer and turbulent simulation of nanomaterial due to compound turbulator including irreversibility analysis. Int J Heat Mass Transf. 2019;137:1290–300.
8. Selimefendigil F, Öztop HF. Laminar convective nanofluid flow over a backward-facing step with an elastic bottom wall. J Thermal Sci Eng Appl. 2017;9(2):021016.
9. Selimefendigil F, Chamkha AJ. Magnetohydrodynamics mixed convection in a power law nanofluid-filled triangular cavity with an opening using Tiwari and Das' nanofluid model. J Therm Anal Calorim. 2019;135(1):419–36.
10. Choi SUS. Enhancing thermal conductivity of fluids with nanoparticles. In: The Proceedings of the 1995 ASME international mechanical engineering congress and exposition, San Francisco. ASME, FED 231/MD, vol. 66; 1995. p. 99–105.
11. Sheremet MA, Oztop HF, Pop I. MHD natural convection in an inclined wavy cavity with corner heater filled with a nanofluid. J Magn Magn Mater. 2016;416:37–47. https://doi.org/10.1016/j.jmmm.2016.04.061.
12. Kefayati GHR. Simulation of heat transfer and entropy generation of MHD natural convection of non-Newtonian nanofluid in an enclosure. Int J Heat Mass Transf. 2016;92:1066–89. https://doi.org/10.1016/j.ijheatmasstransfer.2015.09.078.
13. Kefayati GHR. Simulation of double diffusive MHD (magnetohydrodynamic) natural convection and entropy generation in an open cavity filled with power-law fluids in the presence of Soret and Dufour effects (part I: study of fluid flow, heat and mass transfer). Energy. 2016;107:889–916. https://doi.org/10.1016/j.energy.2016.05.049.
14. Sheikholeslami M, Sheremet MA, Shafee A, Li Z. CVFEM approach for EHD flow of nanofluid through porous medium within a wavy chamber under the impacts of radiation and moving walls. J Therm Anal Calorim. 2019. https://doi.org/10.1007/s10973-019-08235-3.
15. Sheikholeslami M, Arabkoohsar A, Khan I, Shafee A, Li Z. Impact of Lorentz forces on Fe_3O_4–water ferrofluid entropy and exergy treatment within a permeable semi annulus. J Clean Prod. 2019;221:885–98.
16. Sheikholeslami M, Keramati H, Shafee A, Li Z, Alawad OA, Tlili I. Nanofluid MHD forced convection heat transfer around the elliptic obstacle inside a permeable lid drive 3D enclosure considering lattice Boltzmann method. Phys A. 2019;523:87–104.
17. Sheikholeslami M, Rokni HB. Numerical modeling of nanofluid natural convection in a semi annulus in existence of Lorentz force. Comput Methods Appl Mech Eng. 2017;317:419–30. https://doi.org/10.1016/j.cma.2016.12.028.
18. Sheikholeslami M, Shafee A, Zareei A, Haq RU, Li Z. Heat transfer of magnetic nanoparticles through porous media including exergy analysis. J Mol Liq. 2019;279:719–32.
19. Selimefendigil F, Oztop HF. Fluid-solid interaction of elastic-step type corrugation effects on the mixed convection of nanofluid in a vented cavity with magnetic field. Int J Mech Sci. 2019;152:185–97.
20. Rashad AM, Rashidi MM, Lorenzini G, Ahmed SE, Aly AM. Magnetic field and internal heat generation effects on the free convection in a rectangular cavity filled with a porous medium saturated with Cu–water nanofluid. Int J Heat Mass Transf. 2017;104:878–89. https://doi.org/10.1016/j.ijheatmasstransfer.2016.08.025.
21. Sheikholeslami M, Jafaryar M, Shafee A, Li Z, Haq RU. Heat transfer of nanoparticles employing innovative turbulator considering entropy generation. Int J Heat Mass Transf. 2019;136:1233–40.
22. Farshad SA, Sheikholeslami M. Simulation of exergy loss of nanomaterial through a solar heat exchanger with insertion of multi-channel twisted tape. J Therm Anal Calorim. 2019. https://doi.org/10.1007/s10973-019-08156-1.
23. Rashidi S, Javadi P, Esfahani JA. Second law of thermodynamics analysis for nanofluid turbulent flow inside a solar heater with the ribbed absorber plate. J Therm Anal Calorim. 2018. https://doi.org/10.1007/s10973-018-7070-9.
24. Sheikholeslami M, Haq RU, Shafee A, Li Z, Elaraki YG, Tlili I. Heat transfer simulation of heat storage unit with nanoparticles and fins through a heat exchanger. Int J Heat Mass Transf. 2019;135:470–8.
25. Sheikholeslami M, Shehzad SA. Magnetohydrodynamic nanofluid convective flow in a porous enclosure by means of LBM. Int J Heat Mass Transf. 2017;113:796–805.
26. Sheikholeslami M, Mahian O. Enhancement of PCM solidification using inorganic nanoparticles and an external magnetic field with application in energy storage systems. J Clean Prod. 2019;215:963–77.
27. Sheikholeslami M, Jafaryar M, Shafee A, Li Z. Nanofluid heat transfer and entropy generation through a heat exchanger considering a new turbulator and CuO nanoparticles. J Therm Anal Calorim. 2019. https://doi.org/10.1007/s10973-018-7866-7.
28. Sheikholeslami M, Mehryan SAM, Shafee A, Sheremet MA. Variable magnetic forces impact on Magnetizable hybrid nanofluid heat transfer through a circular cavity. J Mol Liq. 2019;277:388–96.
29. Bellos E, Tzivanidis C. Thermal efficiency enhancement of nanofluid-based parabolic trough collectors. J Therm Anal Calorim. 2018. https://doi.org/10.1007/s10973-018-7056-7.
30. Sheikholeslami M. New computational approach for exergy and entropy analysis of nanofluid under the impact of Lorentz force through a porous media. Comput Methods Appl Mech Eng. 2019;344:319–33.
31. Arul Kumar R, Ganesh Babu B, Mohanraj M. Thermodynamic performance of forced convection solar air heaters using pin-fin absorber plate packed with latent heat storage materials. J Therm Anal Calorim. 2016;126:1657–78.
32. Meibodi SS, Kianifar A, Mahian O, Wongwises S. Second law analysis of a nanofluid-based solar collector using experimental data. J Therm Anal Calorim. 2016;126:617–25.
33. Sheikholeslami M, Barzegar Gerdroodbary M, Moradi R, Shafee A, Li Z. Application of neural network for estimation of heat transfer treatment of Al_2O_3–H_2O nanofluid through a channel. Comput Methods Appl Mech Eng. 2019;344:1–12.
34. Sheikholeslami M. Application of control volume based finite element method (CVFEM) for nanofluid flow and heat transfer. Amsterdam: Elsevier; 2019.
35. Rokni HB, Moore JD, Gupta A, McHugh MA, Gavaises M. Entropy scaling based viscosity predictions for hydrocarbon mixtures and diesel fuels up to extreme conditions. Fuel. 2019;241:1203–13.
36. Rashidi S, Eskandarian M, Mahian O, Poncet S. Combination of nanofluid and inserts for heat transfer enhancement. J Therm Anal Calorim. 2018. https://doi.org/10.1007/s10973-018-7070-9.
37. Jafaryar M, Sheikholeslami M, Li Z, Moradi R. Nanofluid turbulent flow in a pipe under the effect of twisted tape with alternate axis. J Therm Anal Calorim. 2018. https://doi.org/10.1007/s10973-018-7093-2.
38. Sun F, Yao Y, Li X, Li G, Miao Y, Han S, Chen Z. Flow simulation of the mixture system of supercritical CO_2 & superheated steam in toe-point injection horizontal wellbores. J Petrol Sci Eng. 2018;163:199–210.

39. Rokni HB, Gupta A, Moore JD, McHugh MA, Bamgbaded BA, Gavaises M. Purely predictive method for density, compressibility, and expansivity for hydrocarbon mixtures and diesel and jet fuels up to high temperatures and pressures. Fuel. 2019;236:1377–90.
40. Saravia CM. A formulation for modelling levitation based vibration energy harvesters undergoing finite motion. Mech Syst Signal Process. 2019;117:862–78.
41. Sheikholeslami M, Zeeshan A. Analysis of flow and heat transfer in water based nanofluid due to magnetic field in a porous enclosure with constant heat flux using CVFEM. Comput Methods Appl Mech Eng. 2017;320:68–81.
42. Yadav D, Wang J, Bhargava R, Lee J, Cho HH. Numerical investigation of the effect of magnetic field on the onset of nanofluid convection. Appl Therm Eng. 2016;103:1441–9.
43. Sheikholeslami M, Haq RU, Shafee A, Li Z. Heat transfer behavior of Nanoparticle enhanced PCM solidification through an enclosure with V shaped fins. Int J Heat Mass Transf. 2019;130:1322–42.
44. Stalin PMJ, Arjunan TV, Matheswaran MM, Sadanandam N. Experimental and theoretical investigation on the effects of lower concentration CeO_2/water nanofluid in flat-plate solar collector. J Therm Anal Calorim. 2017. https://doi.org/10.1007/s10973-017-6865-4.
45. Qi C, Wang G, Yan Y, Mei S, Luo T. Effect of rotating twisted tape on thermo-hydraulic performances of nanofluids in heat-exchanger systems. Energy Convers Manag. 2018;166:744–57.
46. Sheikholeslami M. Numerical approach for MHD Al_2O_3–water nanofluid transportation inside a permeable medium using innovative computer method. Comput Methods Appl Mech Eng. 2019;344:306–18.
47. Zheng S, Juntai S, Keliu W, Xiangfang L. Gas flow behavior through inorganic nanopores in shale considering confinement effect and moisture content. Ind Eng Chem Res. 2018;57:3430–40.
48. Sheikholeslami M, Shehzad SA, Li Z, Shafee A. Numerical modeling for alumina nanofluid magnetohydrodynamic convective heat transfer in a permeable medium using Darcy law. Int J Heat Mass Transf. 2018;127:614–22.
49. Alkanhal TA, Sheikholeslami M, Usman M, Haq RU, ShafeeA Al-Ahmadi AS, Tlili I. Thermal management of MHD nanofluid within the porous medium enclosed in a wavy shaped cavity with square obstacle in the presence of radiation heat source. Int J Heat Mass Transf. 2019;139:87–94.